

# Dynamics and Control of Accumulators in Continuous Strip Processing Lines

P. R. Pagilla, S. S. Garimella, L. H. Dreinhofer, E. O. King

**Abstract**—Accumulators in a strip processing line are primarily used to allow for rewind or unwind core change while the process continues at a constant velocity. Accumulators facilitate continuous operation of the process line and thus constitute an important element of a continuous strip processing line. This paper studies the coupled dynamics of the accumulator carriage motion, rollers and web spans. Suggestions are made in an effort to integrate the tension dynamics of individual spans in an accumulator. An average dynamic model that integrates the dynamic models of individual spans in the accumulator is derived. This aggregation of the dynamics can facilitate control design for the accumulator carriage. Hydraulic system modeling associated with the accumulator is studied. Aspects of the hydraulic system such as drop due to friction in long pipes and dominant damped resonant frequency of the hydraulic system are discussed. A compact state space model of the dynamic model of the accumulator is obtained from the average span tension dynamics, carriage dynamics, and pressure dynamics. Some experiments conducted on an Alcoa continuous process line are discussed.

**Keywords**— Accumulators, aluminum strip processing, dynamic modeling, tension control, hydraulic systems.

## I. INTRODUCTION

Maintaining strip tension in the accumulator spans while the accumulator carriage moves up/down is essential to maintaining tension in the entire strip processing line. It has been observed on an Alcoa finishing process line that the dynamics of the accumulator plays an important role on the behavior of strip tension in the entire line. Tension disturbance propagation has been observed due to motion of the accumulator carriage both upstream and downstream of the accumulator. A sketch of an exit accumulator in a continuous aluminum strip processing line is shown in Fig. 1, and Fig. 3 illustrates the hydraulic system of the accumulator. Motion of the accumulator carriage is facilitated by the change in strip velocity between the process and exit side of the accumulator. Further, the accumulator carriage is loaded by a force using a hydraulic system (ram

and cylinder) in opposition to the tension from the multiple strands of strips in accumulator spans.

The primary motivation for this work stems from the observations made on an Alcoa Continuous strip Processing Line (CPL). The focus of this work is on the accumulator aspects of the CPL. It has been observed that the friction between the ram and the cylinder during carriage motion plays a major role in the strip tension change through the accumulator. For example, friction for up and down motion is different. Seal design and rod lubrication are big factors. Specific loss compensation is required to avoid disturbance to the sheet tension during carriage motion. Loss compensation is done by either raising or lowering the reference pressure in the cylinders. A technique that can provide the amount of loss compensation and when it should be applied is useful. Further, break away friction prevents the ram from moving on small sheet tension variations. This results in an undesirable consequence of passing tension changes through the accumulator. Also, the large mass of the carriage and rolls limit the accumulator ability to respond to higher frequency sheet tension disturbances. Roller bearing friction is also a major factor in the tension change through the accumulator. Typical accumulators have 20 or more rollers. Therefore, bearing lubrication is important.

Resonance characteristics of the cylinder and carriage play an important role in sheet tension variations. A low frequency resonance in the 1 to 5 Hz range is undesirable as some of the line sheet spans are also resonant in this region. Carriage position effects the volume of the fluid in the cylinder which also effects the stability of the pressure controller. Prior work to alleviate some of these effects involved de-tuning of the pressure regulator, which has proven helpful in allowing for a more stable operation of the full range of cylinder positions. This also reduced oscillations being driven into nearby resonant sheet spans. This work builds on the prior research of the authors which appeared in unpublished reports [1], [2], [3]. Length of a web span within an accumulator varies over a wide range as the carriage moves up and down. Some of the authors prior work reported in [8] developed a dynamic model for accumulator spans that considers the time-varying nature of the span length. A large body of research in modeling

This work was supported by ALCOA.  
P.R. Pagilla is with the School of Mechanical and Aerospace Engineering, Oklahoma State University, Stillwater, OK.  
S.S. Garimella and E.O. King are with ALCOA Technical Center, Pittsburgh, PA.  
L.H. Dreinhofer is with ALCOA FRP Engineering, Knoxville, TN.

and control of web handling systems can be found in [4], [5], [6], [7] and references therein. Earlier work in dynamics and control of hydraulic systems can be found in the classical text [9]. In [10], criteria for design and selection of hydraulic components is given. A new model for control of systems with friction is discussed in [11].

In this paper, a dynamic model for the accumulator system that includes carriage dynamics, web span dynamics, and fluid pressure dynamics is developed. Since the accumulator contains a large number of web spans and rollers, an aggregate dynamic model that integrates all the web spans in an average sense has been developed. Speed changes during rewind roll change and its effects on carriage motion are discussed. Hydraulic system of the accumulator is discussed. Specifically, pressure drop due to friction in the long pipe from the valve to the cylinder and dominant damped resonant frequency of the system have been calculated. Some experiments carried out on an Alcoa CPL are discussed.

The rest of the paper is organized as follows. Section II gives the equations of motion of the carriage and web spans. Hydraulic system is discussed in section III. State space form of the accumulator dynamics that includes carriage dynamics, sheet tension dynamics and pressure dynamics, is given in section IV. Some accumulator experiments are discussed in section V. Section VI gives concluding remarks and future research directions.

## II. DYNAMICS OF CARRIAGE AND WEB SPANS

A schematic of the carriage, web spans and rollers within an accumulator is shown in Fig. 1. The accumu-

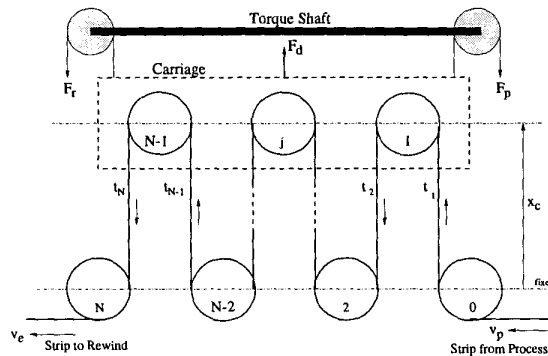


Fig. 1. Sketch of an Exit Accumulator

lator carriage dynamics is given by

$$M_c \frac{d^2 x_c(t)}{dt^2} = F_h(t) - F_d(t) - M_c g - \sum_{j=1}^N t_j(t) \quad (1)$$

where

- $M_c$  carriage mass;
- $x_c$  carriage position;
- $v_c$  carriage velocity ( $= \dot{x}_c$ );
- $F_h$  controlled force,  $F_h = F_r + F_p$ ;
- $F_d$  disturbance force;
- $g$  acceleration due to gravity;
- $N$  number of spans;
- $t_j$  strip tension in the  $j$ -th span;
- $R$  roller radius.

The controlled force,  $F_h(t)$ , is generated by a hydraulic system. Fig. 3 shows a schematic of the hydraulic system. The disturbance force,  $F_d(t)$ , includes the friction in the hydraulic cylinder and the rod seals, friction in the carriage guides and the force due to carriage chain elasticity. The torque shaft shown in Fig. 1 is included in the accumulator design to synchronize the side to side lifting action so that only vertical motion needs to be considered in the control system design. The number of rollers on the carriage is  $N/2$ . The number of rollers in the accumulator is  $N + 1$ . The strip tension and the roller dynamics in the  $j$ -th accumulator span is given by [8], [7],

$$\begin{aligned} \frac{dt_j(t)}{dt} = & \frac{AER}{x_c(t)} (\omega_j(t) - \omega_{j-1}(t)) \\ & + \frac{R}{x_c(t)} [t_{j-1}(t)\omega_{j-1}(t) - t_j(t)\omega_j(t)] \\ & + \frac{AE}{x_c(t)} \dot{x}_c(t) - \frac{1}{x_c(t)} t_j(t) \dot{x}_c(t) \end{aligned} \quad (2)$$

$$J \frac{d\omega_j(t)}{dt} = -B_j \omega_j + R(t_{j+1}(t) - t_j(t)) \quad (3)$$

where  $j = 1 : N$ , and

- $A$  area of cross-section of the strip;
- $E$  modulus of elasticity of the strip;
- $R$  radius of the roller;
- $\omega_j$  angular velocity of the  $j$ -th roller;
- $J$  moment of inertia of the roller;
- $B_j$  viscous friction coefficient of the  $j$ -th roller;

Notice that there is a strong coupling between the carriage dynamics (1), strip tension dynamics (2), and the roller dynamics (3).

### A. Speed changes during rewind roll change

A typical scenario of the exit speed and the carriage speed during a rewind roll change is depicted in Fig. 2. The following steps describe a rewind roll change-over scenario when the strip velocity in the process section is maintained at a constant value: (i) AB - velocity of the strip in the rewind side is decelerated to zero, as a result of this the accumulator starts collecting strip and the carriage

accelerates upwards; (ii) BC – rewind stops and the carriage is moving up with constant velocity; (iii) CD – after rewind roll change, exit side is accelerated up to the process speed, in this period the carriage is moving up while decelerating; (iv) DF – exit side is accelerated up to a speed above the process speed; (v) EF – exit speed is maintained at a constant speed; (vi) FG – exit speed is reduced to the process speed. The carriage after this cycle returns to its original position. Notice that carriage returns to its original position when the area under the carriage speed graph of Fig. 2 is zero.

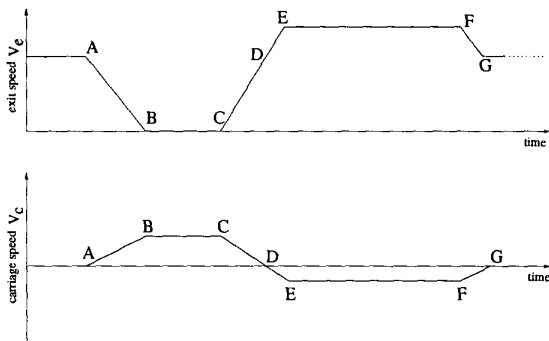


Fig. 2. Exit and Carriage Speeds during Roll-change

Since there are  $N$  spans in the accumulator, carriage velocity can be obtained based on the process speed and the exit speed, under the assumption that there is no web slippage on the rollers. The relationship between the process speed,  $v_p$ , the exit speed,  $v_e$ , and the carriage speed in an ideal situation is given by the following:

$$v_c = \frac{v_p - v_e}{N} \quad (4)$$

$$\omega_j = \frac{v_p - jv_c}{R} \quad (5)$$

It is assumed in this paper that the process speed is the speed of the strip in the span just upstream of the accumulator, as shown in Fig. 1, and the exit speed is the speed of the strip in the span just downstream of the accumulator. The carriage speed, (4), depends on the speed variation between the process section and the exit section. Generally, the process speed is kept constant and the exit speed varies according to the sketch shown in Fig. 2. When the strip is stationary at the exit side of the accumulator,  $v_e = 0$ , then equations (4) and (5) become

$$v_c = \frac{v_p}{N} \quad (6)$$

$$\omega_j = \frac{v_c}{R}(N - j) \quad (7)$$

Using this notion of speed changes at the exit side, some observations can be drawn from the dynamics of the carriage, (1). Assume that the external disturbance force,  $F_d(t)$ , is zero. If the web is stationary at the exit side then the carriage is moving up with a constant velocity, i.e., carriage acceleration is zero, then (1) becomes

$$F_h(t) = M_c g + \sum_{j=1}^N t_j(t) \quad (8)$$

Further, from (7) the angular acceleration of each roller is zero. As a result of this, (3) gives  $t_j = t_{j+1}$  for all  $j = 1 : N$ . This is true under the assumption that the roller bearing friction,  $B_j$ , is zero. If  $B_j$  is non-zero, then there is a loss in tension, which is ignored assuming it is small for the analysis in this section. Thus, when the exit side is stationary, the tensions in the spans are equal and the controlled force is required to overcome the weight of the carriage, sum of the tensions in the spans, and other force disturbances. Now consider the scenario of constant acceleration or deceleration of the exit side and constant process speed. The carriage dynamics, (1), can be re-written as,

$$F_h(t) = M_c \frac{dv_c}{dt} + M_c g + \sum_{j=1}^N t_j(t) \quad (9)$$

It should be observed that during deceleration of the exit side, the carriage is accelerating up, i.e.,  $dv_c/dt$  is positive. Hence, the controlled force,  $F_h(t)$ , in this case should be larger than the controlled force when the exit side is stationary. However, in the event of acceleration of the exit side,  $dv_c/dt$  is negative, and hence the controlled force  $F_h(t)$  in this case is smaller than the one required for the stationary exit side case.

### B. Aggregation of dynamics

The motivation for averaging the tension dynamics of  $N$  web spans in the accumulator is to obtain a simpler dynamic model for all the accumulator spans in an average sense. Consider a new variable  $t_c$ , which denotes an average sum of the tensions in the accumulator web spans and is given by

$$t_c(t) = \frac{1}{N} \sum_{j=1}^N t_j(t) \quad (10)$$

Taking the sum from  $j = 1$  to  $j = N$  of both sides of (2) and dividing by  $N$  results in

$$\begin{aligned} \frac{dt_c(t)}{dt} &= \frac{AER}{x_c(t)} \frac{1}{N} \sum_{j=1}^N (\omega_j(t) - \omega_{j-1}(t)) \\ &+ \frac{1}{N} \sum_{j=1}^N \frac{R}{x_c(t)} (t_{j-1}(t)\omega_{j-1}(t) - t_j(t)\omega_j(t)) \\ &+ \frac{1}{N} \sum_{j=1}^N \frac{AE}{x_c(t)} \dot{x}_c(t) - \frac{1}{N} \sum_{j=1}^N \frac{1}{x_c(t)} t_j(t) \dot{x}_c(t) \end{aligned} \quad (11)$$

Evaluating the sum on the right-hand-side results in

$$\begin{aligned} \frac{dt_c(t)}{dt} &= \frac{AER}{x_c(t)} \frac{1}{N} (\omega_N(t) - \omega_0(t)) \\ &+ \frac{1}{N} \frac{R}{x_c(t)} (t_0(t)\omega_0(t) - t_N(t)\omega_N(t)) \\ &+ \frac{AE}{x_c(t)} \dot{x}_c(t) - \frac{1}{x_c(t)} t_c(t) \dot{x}_c(t) \end{aligned} \quad (12)$$

Using this approach, the average dynamics in terms of  $t_c(t)$  simplifies the dynamics of  $N$  spans given by  $N$  equations of (2). Notice that the average dynamics, (12), simply looks like the strip tension dynamics of an accumulator with a single roller on its carriage. Also, notice that the last summation in the carriage dynamics, (1), can be replaced with  $Nt_c(t)$ . Further simplification of the average dynamics, (12), is possible by assuming that  $N$  is large. For a typical ALCOA accumulator considered in this paper, the value of  $N$  is 34. Using this assumption, the second term in equation (12) is small compared to other terms. Ignoring the second term results in the following average dynamics.

$$\begin{aligned} \frac{dt_c}{dt} &= \frac{AER}{x_c(t)} \frac{1}{N} (\omega_N(t) - \omega_0(t)) \\ &+ \frac{AE}{x_c(t)} \dot{x}_c(t) - \frac{1}{x_c(t)} t_c(t) \dot{x}_c(t) \end{aligned} \quad (13)$$

Notice that the process velocity is  $v_p = R\omega_0$  and from (5),  $\omega_N = (v_p - Nv_c)/R$ . Therefore,

$$\omega_N - \omega_0 = -N \frac{v_c}{R} \quad (14)$$

Since  $v_c = \dot{x}_c$ , substituting (14) into (13) gives

$$\frac{dt_c(t)}{dt} = -\frac{1}{x_c(t)} t_c(t) \dot{x}_c(t) \quad (15)$$

The carriage dynamics, (1), can be re-written as

$$M_c \frac{d^2 x_c(t)}{dt^2} = F_h(t) - F_d(t) - M_c g - t_c(t) \quad (16)$$

Together, equations (15) and (16) characterize the dynamics of the accumulator carriage and its spans in an average sense. This dynamic model is suitable for design of the controller force,  $F_h(t)$ , to provide a desired regulation of the average tension in the accumulator spans. The control force  $F_h(t)$  is generated by a hydraulic system, which is discussed in the next section.

### III. HYDRAULIC SYSTEM

A schematic of the accumulator hydraulic system and the carriage is shown in Fig. 3. It consists of two symmetrically placed cylinders, a directional proportional valve, and a pressure compensated pump. The pressure in each cylinder is regulated by the same directional proportional valve.

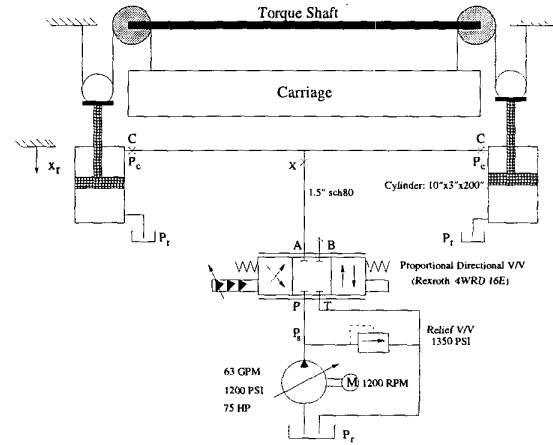


Fig. 3. Accumulator Hydraulic System

#### A. Pressure drop in the pipe

Since the pipe length from the proportional valve (point A) to the entry point of the cylinder (point  $P_c$ ) is generally large, as in the case of Alcoa CPL, pressure drop due to pipe length and bends is calculated in this section. All calculations are based on an Alcoa CPL. The following values are used in the calculations:

$$\begin{aligned} A_{cyl} &= 71.5 \text{ in}^2, \text{ rod-side cylinder area;} \\ V_r &= 1.65 \text{ in/s, ram velocity } (= Q_s/A_{cyl}); \\ D_{in} &= 1.5 \text{ in, pipe inner diameter;} \\ \rho &= 8.05 \times 10^{-5} \text{ lbf} \cdot \text{s}^2 \cdot \text{in}^{-4}, \\ &\text{density of fluid;} \\ \mu &= 8.5 \times 10^{-6} \text{ lbf} \cdot \text{s} \cdot \text{in}^{-2}, \\ &\text{absolute viscosity.} \end{aligned}$$

Calculation of the Reynolds number for rated flow through the pipes shows that the fluid flow is in the laminar

region. The Reynolds number calculation is done using the expression

$$N_R = \frac{\rho u D}{\mu} \quad (17)$$

where  $u$  is the fluid velocity in the pipe, It is assumed that the pressure compensated pump maintains a constant pressure of 1200 PSI to the inlet of the proportional valve. The pressure energy losses due to friction can be calculated using Darcy's empirical formula [10], which is

$$\Delta P = f_D \frac{L \rho}{2D} \left( \frac{Q_s}{A_{cyl}} \right)^2 = \frac{f_D L \rho u^2}{2D} \quad (18)$$

where  $\Delta P$  is the pressure drop in the pipe,  $f_D$  is the dimensionless friction factor,  $Q_s$  is the rated flow rate through the pipe and  $L$  is the length of the pipe considering bends and elbows. The straight length of the pipe measured from the proportional valve to the entry point of each cylinder is 506 inches. The friction factor when the flow is laminar, i.e., Reynolds number less than 2000, can be found by equating Darcy's pressure drop expression (18) with Hagen-Poiseuille law, which is

$$\Delta P = \frac{128 \mu L Q_s}{\pi D^4} \quad (19)$$

For laminar flow, the friction factor is  $64/N_R$ . Since there are three 90 degree elbows in the pipe between points A and X, the equivalent length for these elbows is calculated as

$$L_e = \frac{K D}{f_D} = \frac{3 K D N_R}{64}$$

Assuming  $K = 1.12$  for each 90 degree elbow,  $L_e = 153.92''$ . Therefore, the total effective length between points A and X on the pipe is given by  $L = 14'' + 48'' + 64'' + L_e = 385.92''$ . The pressure drop is given by

$$P_A - P_x = 6.4 \text{ PSI}$$

For the section between points X and the cylinder entrance, the constant  $K$  (3 x elbow + 1 x tee) due to one tee joint and three 90 degree elbow joints is  $K = 3.36 + 1.2 = 4.56$ . The equivalent length is  $L_e = 104.5''$ . Therefore, the pressure drop from point X to the entry of the cylinder is given by

$$P_x - P_c = 3.1 \text{ PSI}$$

Thus, the pressure drop, due to friction in the pipes, between the exit side of the proportional valve and entry of the cylinder is approximately 9.4 PSI, which is very small compared to the reference pressure of 780 PSI.

### B. Dominant damped resonant frequency

The resonant frequency of the cylinder is computed using the following expression,

$$\omega_{cyl} = \sqrt{\frac{\beta A_{cyl}^2}{m_{refl} V}} \quad (20)$$

where  $\beta$  is the bulk modulus of the fluid,  $V$  is the pipe and cylinder volume, and  $m_{refl}$  is the reflected or equivalent mass calculated from the force due to reference pressure in the cylinder, which is

$$m_{refl} = \frac{2 P_c A_{cyl}}{g} = 285.3 \text{ lbs}$$

The total volume of the fluid in the cylinder and pipe is

$$V = \frac{\pi}{4} D^2 L + A_{cyl} h_{cyl} = 893.7 + 15188.2 \text{ in}^3$$

where  $h_{cyl}$  is the height of the cylinder or ram stroke, which is equal to 200 inches. Using these numbers, the damped frequency,  $\omega_L$ , is 13.3 rad/s or 2.1 Hz. The resonant frequency of the proportional valve is 35 Hz. Thus, the dominant damped resonance is at 2.1 Hz. The low value of the dominant resonant frequency is mainly due to the long ram stroke in the cylinder. This leads to low system rigidity, which may result in poor response of the ram to accelerations and decelerations. Further, stick-slip can be expected at low travel speeds of the ram.

### C. Dynamic model of the hydraulic system

The dynamic pressure-flow equation in the cylinders is governed by

$$\sum Q_{in} - \sum Q_{out} = \frac{V_o}{\beta} \frac{dP}{dt} + A_{cyl} \frac{dx_r}{dt} \quad (21)$$

where  $Q_{in}$  ( $Q_{out}$ ) is the flow entering (leaving) the system,  $V_o$  is the fluid volume,  $\beta$  is the bulk modulus of the fluid,  $P$  is the system pressure, and  $x_r$  is the ram displacement. For the cylinder set up shown in Fig. 3, the cylinder pressure dynamics can be simplified to

$$\frac{V_o}{\beta} \frac{dP_c(t)}{dt} = Q_c(t) - C_m(P_c(t) - P_r) - A_{cyl} \dot{x}_r(t) \quad (22)$$

where  $Q_c(t)$  is the flow rate to and from the cylinder, which is related to the proportional spool-valve displacement  $x_v$  by

$$Q_c(t) = K_q x_v \sqrt{P_s - P_c(t)} \quad \text{for } x_v > 0 \quad (23)$$

$$Q_c(t) = K_q x_v \sqrt{P_c(t) - P_r} \quad \text{for } x_v < 0 \quad (24)$$

and

- $V_0(t)$  total control volume in the rod-side cylinder chamber;
- $C_m$  coefficient of internal leakage of the cylinder;
- $P_c(t)$  cylinder pressure;
- $P_r$  return pressure (= 200 PSI);
- $P_s$  supply pressure (= 1200 PSI);
- $A_{cyl}$  rod-side cylinder area;
- $x_r(t)$  ram displacement;
- $K_q$  flow gain coefficient.

The total control volume is  $V_0(t) = V_{in} + A_{cyl}x_r(t)$ , where  $V_{in}$  is the initial volume of the cylinder when the ram is fully extended, i.e., when  $x_r = 0$ . Due to the pulley system as shown in Fig. 3, the ram displacement is exactly half of the carriage displacement,  $x_r(t) = 0.5x_c(t)$ . The position of the ram,  $x_r(t)$ , is positive downwards as shown in Fig. 3, whereas the position of the carriage,  $x_c(t)$ , is positive upwards.

#### IV. ACCUMULATOR DYNAMICS

Considering the pressure in each cylinder to be the same, i.e.,  $P_c(t)$ , the force on the carriage is  $F_h(t) = P_c(t)A_{cyl}$ . Using this expression for controlled force, equations (15), (16), (22) can be combined into the state space form. Define the state variables,  $\xi_1(t) = t_c(t)$ ,  $\xi_2(t) = x_c(t)$ ,  $\xi_3(t) = v_c(t)$ ,  $\xi_4(t) = P_c(t)$  and input,  $u = x_v$ . Consider the disturbance force,  $F_d(t)$ , to be only due to friction in the cylinder, i.e.,  $F_d(t) = F_f(\xi_3)$ . Then, the state space form of the dynamics is

$$\dot{\xi}_1 = -\frac{\xi_3}{\xi_2}\xi_1 \quad (25)$$

$$\dot{\xi}_2 = \xi_3 \quad (26)$$

$$\dot{\xi}_3 = \frac{1}{M_c}(-\xi_1 - F_f(\xi_3) + A_{cyl}\xi_4) - g \quad (27)$$

$$\dot{\xi}_4 = \alpha(\xi_2) \left( -\frac{A_{cyl}}{2}\xi_3 - C_m(\xi_4 - P_r) \right) + g(\xi_4, u)u \quad (28)$$

where  $\alpha(\xi_2) = \beta/(V_{in} + A_{cyl}\xi_2)$ ,  $g(\xi_4, u)$  is obtained from (23), (24) and can be written as a single function that includes both spool-valve directions as

$$g(\xi_4, u) = \frac{K_q}{2}(1 + \text{sgn}(u))\sqrt{P_s - \xi_4} + \frac{K_q}{2}(1 - \text{sgn}(u))\sqrt{\xi_4 - P_r} \quad (29)$$

where  $\text{sgn}(u)$  is the sign function. Since a considerable amount of stick-slip is observed during ram movement in the cylinder, viscous and Coulomb friction force

model can be used for  $F_f(\xi_3)$ , that is  $F_f(\xi_3) = -v_f\xi_3 - c_f\text{sgn}(\xi_3)$ , where  $v_f$  is the viscous friction coefficient and  $c_f$  is the Coulomb friction coefficient.

#### V. ACCUMULATOR TESTS

When the carriage is stationary, the fluid pressure in the cylinders is regulated at a constant reference pressure of  $P_{ref} = 780$  PSI. Since there are 34 spans in the accumulator and the carriage weight is 16,134 lbs, the reflected sheet tension is 1165 lbs. In the current operation, when the accumulator is moving up, the reference pressure is increased by a constant amount to maintain sheet tension. Tests were conducted on the accumulator in an effort to explain the increase in reference pressure required to maintain tension. In the following, this increase in reference pressure will be referred to as pressure boost ( $\Delta P_{ref}$ ). The pressure boost is active whenever the process speed exceeds exit speed by 25 FPM, i.e.,  $v_p - v_e \geq 25$  FPM.

Experimental data is recorded on an Alcoa CPL for various levels of pressure boost. The pressure reference,  $P_{ref} = 780$  PSI, is kept the same throughout the data collection whereas the pressure boost,  $\Delta P_{ref}$ , is varied. The exit accumulator load cell variations ( $\Delta T$ ) for different boost pressures are given in the following table.

Pressure boost ( $\Delta P_{ref}$ ) (PSI)	Load cell $\Delta T$ (lbs)
0	- 319
66	- 174
115	- 116
165	0
215	+ 116
265	+ 203
315	+ 348

A reasonable explanation of the pressure boost when the accumulator is moving up is to account for friction in the cylinder and rod seals and to compensate for the acceleration component of the carriage given by (9). This can be validated from the data recorded when there is no pressure boost, i.e.,  $\Delta P_{ref} = 0$ . From the data when  $\Delta P_{ref} = 0$ , there is an instantaneous drop in the sheet tension equal to 319 lbs, when the carriage starts to move up. The ram is fully extended when the carriage is at its bottom position. As the dry ram moves into the cylinder the accumulator starts moving up. Dry breakaway friction may cause such sudden drop in sheet tension when carriage starts to move up.

The load cell reading shows an instantaneous jump (data not shown) as soon as the exit speed exceeds the process speed, i.e., carriage starts to move down, and the reference pressure boost is no longer required. Also, there

is no appreciable drop in tension when the accumulator is moving down. This may be due to the fact that the ram coming out of the cylinder is well lubricated. Further, the seals may have low friction when the ram is moving out of the cylinder, and high friction when the rod is moving into the cylinder. Since pressure boost is required only when the carriage is moving up, it appears that the requirement of additional force to compensate for acceleration may not be significant when compared to frictional force. Further, more experiments need to be carried out at low speeds and different rates of variation of the exit and process speed to confirm these predictions.

## VI. CONCLUSION AND FUTURE WORK

In this paper, a dynamic model for the accumulator that includes sheet tension dynamics, carriage dynamics and pressure dynamics is developed. Understanding the effects of sheet tension variation when the sheet passes through an accumulator is important before finding ways to control and minimize such variations. Throughout this paper suggestions and remarks are made to address this issue and draw more insights into the problem. As a result, this work provides a good background to future research on accumulators.

It is evident that considerable work needs to be done to better explain a number of issues that were discussed in the introduction section. An immediate issue is to design an efficient control algorithm for the dynamic model of the accumulator. Currently, PID based control strategies are extensively used in the industry. These strategies are easy to tune and develop, but have their own limitations in system performance and robustness. Further, the dynamic model of the accumulator is highly nonlinear, especially the pressure dynamics given by (28), which may lead to undesirable performance. So, if tighter control and better performance is sought, then clever augmentation of PID based strategies should be considered, which will be the focus of our future work.

It is also evident that friction is a major factor, wherever it may be in the accumulator system, i.e., cylinder walls, seals, rollers, carriage guides, etc. Therefore, study of friction in the accumulator system is important. Although a friction model that includes linear viscous friction and Coulomb friction is proposed in section IV, it is quite conceivable that better friction modeling may be required for accumulators that have some of the peculiar friction characteristics mentioned in the introduction. Perhaps, dynamic friction models that are considered in [11] and some of its references can predict better accumulator friction characteristics. Future research focus can look at fitting some of the dynamic friction models to the accu-

mulator friction characteristics observed in experiments. Another aspect is to consider alternative technologies such as use of DC motor to pull tension on the carriage instead of the hydraulic system. The DC motor must be oversized or external force cooled to allow required currents at zero motor speed. Use of AC motor with vector torque regulators is another possible alternative to drive the carriage. The AC motor can be smaller than the DC motor but still requires external forced cooling.

Finally, there is a need to conduct experiments on a CPL with a well designed experimental procedure. This can better validate the concepts developed and provide directions to iterate on these concepts to better model and control the dynamic behavior.

## ACKNOWLEDGMENTS

The authors would like to thank Jim Rushing of Alcoa, Knoxville, Price Philips, Larry Clarke and Dennis Pepper of Alcoa, Warrick, for discussions relating to the continuous process line and also in collecting experimental data.

## REFERENCES

- [1] S.S. Garimella, "A study on dynamic modeling of accumulators," Technical report, ALCOA, Pittsburgh, PA, 1998.
- [2] E.O. King, "Analysis and discussion of experiments conducted on continuous strip processing line," Technical report, ALCOA, Pittsburgh, PA, 1998.
- [3] L.H. Dreinhofer and P.R. Pagilla, "A study on accumulator characteristics," Technical report, ALCOA, Knoxville, TN, 1998.
- [4] K.N. Reid, J.J. Shelton and K.C. Lin, "Distributed control of tension in a web transport system," WHRC project report, Oklahoma State University, May 1992.
- [5] J.J. Shelton, "Sensing of web tension by means of roller reaction forces," WHRC project report, Oklahoma State University, May 1992.
- [6] G.E. Young and K.N. Reid, "Lateral and Longitudinal Dynamic Behavior and Control of Moving Webs," *ASME Journal of Dynamic Systems, Measurement, and Control*, Vol. 115, pp. 309-317, June 1993.
- [7] K.H. Shin, "Distributed Control of Tension in Multi-span Web Transport Systems," Ph.D. dissertation, Oklahoma State University, Stillwater, OK, May 1991.
- [8] P.R. Pagilla, E.O. King, L.H. Dreinhofer and S.S. Garimella, "Robust Observer-Based Control of an Aluminum Strip Processing Line," *Proceedings of the 1999 IEEE Industry Applications Society Conference*, Phoenix, AZ, 1999.
- [9] H.E. Merritt, *Hydraulic Control Systems*. John Wiley & Sons, Inc., New York, 1967.
- [10] E.C. Fitch and I.T. Hong, *Hydraulic Component Design and Selection*. Computerized Fluid Power Series, BarDyne, Inc., Stillwater, OK, 1998.
- [11] C. Canudas de Wit, H. Olsson, K.J. Astrom, and P. Lischinsky, "A new model for control of systems with friction," *IEEE Transactions on Automatic Control*, vol. 40, no. 3, 419-425.